Asian Journal of Chemistry; Vol. 35, No. 7 (2023), 1579-1584

ASIAN JOURNAL OF CHEMISTRY

https://doi.org/10.14233/ajchem.2023.27742

Novel Dihydropyrimidinones: Molecular Docking, Synthesis and Anti-Neoplastic Activity

M.P. TORASKAR*, R. CHAURE and S.S. SONTAKKE

Department of Pharmaceutical Chemistry, Bharati Vidyapeeth's College of Pharmacy, Sector 8, C.B.D. Belapur, Navi Mumbai-400614, India

*Corresponding author: E-mail: mrunmayeetoraskar@gmail.com

Received: 10 March 2023; *Accepted*: 13 April 2023; *Published online*: 6 July 2023; AJC-21277

Recent years have showed great interest in the synthesis of pyrimidinone and its applications in medicinal chemistry. Chalcones were synthesized through the Claisen-Schmidt condensation reaction between substituted aldehydes and acetone in the presence of LiOH to produce dihydropyrimidinones, which were then subjected to urea treatment in the presence of strong HCl to give dihydropyrimidinone derivatives. The antiproliferative activity of synthesized components was screened against MCF7 and MCA-MB-231 cancer cell lines. Compound **4A$_1$** was found to have promising anticancer activity against both cell lines. Overall, the approach makes it possible to synthesize dihydropyrimidinones with potential anticancer properties.

Keywords: Dihydropyrimidinones, Anti-Neoplastic activity.

INTRODUCTION

Heterocyclic compounds such as dihydropyrimidinones (DHPMs) and their derivatives are synthesized by contemporary modifications of traditional multi-component processes such as the Biginelli reaction [1-3]. Due to their purportedly diverse biological action, dihydropyrimidinones, heterocycles with a pyrimidine component in the ring nucleus, have recently sparked attention in medicinal chemistry [4,5].

The diverse family of microtubule-based motor proteins known as kinesins is crucial for many essential cellular processes, including the assembly of the mitotic spindle, vesicular trafficking, remodeling of the microtubules, positioning of the subcellular organelles and segregation of the chromosomes in dividing cells [6,7]. Eg5 is a homotetrameric protein belonging to the kinesin-5 family or the bimC (blocked in mitosis) kinesin subfamily [8,9]. It has an N-terminal microtubule motor that is plus-end-directed. Eg5 is overexpressed in numerous proliferative tissues, including leukemia and solid tumors like lung, breast, ovarian, bladder and pancreatic malignancies, while nearly no Eg5 is seen in non-proliferative tissues. As a result, Eg5 is viewed as a prospective target for the treatment of cancer [10-13]. The ability of monastrol (IC_{50} = 30 μM) to permeate cell membranes and trigger mitosis by reversibly and specifically inhibiting Eg5 myosin kinase was initially discovered by Mayer *et al*. [14] in their study. Other bioactive dihydropyrimidinone-containing scaffolds with anti-proliferative action include dimethylenastron [14] and piperastrol [15].

Chalcones are one of the important precursors of many biologically active compounds and are mainly synthesized by the Claisen-Schmidt condensation reaction [16]. Commercially available lithium hydroxide monohydrate ($LiOH·H_2O$) is found to be a novel 'dual activation' catalyst for tandem condensation between ketones and aromatic aldehydes leading to an efficient, easy synthesis of substituted chalcones at room temperature in short times and afforded excellent yields [17]. As a part of ongoing studies aiming to develop new dihydropyrimidinone derivatives as anticancer agents, some novel dihyropyrimidinones from substituted dibenzylidene chalcones on reaction with urea were synthesized and characterized.

EXPERIMENTAL

All the chemicals and solvents were procured from S.D. Fine Chem., India and Sigma-Aldrich, USA. The reagents used were of analytical grade and utilized without further purification, whereas the solvents used were of commercial grade. They were used after purification. Melting points were determined on a VEEGO (VMP-D) melting point apparatus and are uncorrected. ^{1}H NMR was recorded at BRUKER ADVANCE II (800 MHz) in $CDCl_3$ as solvent using TMS as an internal standard. IR (ATR) spectra were recorded on a Quest ATR Diamond

Accessory (Black) P31482 & Shimadzu 8100 infrared spectrophotometer. Mass spectra were recorded at Ambernath organics Pvt Ltd, Mumbai, India.

General procedure

Synthesis of (1*E*,4*E*)-1,5-diphenylpenta-1,4-dien-3-one ($3A_1$-$3A_5$): In a 250 mL conical flask containing a magnetic bar, a mixture of substituted aldehyde (0.113 mol), acetone (0.055 mol) and lithium monohydrate (1.26 g) in 30 mL ethanol was stirred till a yellowish solid mass precipitated out. The reaction mixture was cooled on an ice bath and the solid precipitate was filtered at suction. The crude obtained was washed with cold water, air-dried and recrystallized using ether to obtain pure chalcone [18].

Synthesis of 4-phenyl-6-[(1*E*)-2-phenylethenyl]-1,2,3,4-tetrahydropyrimidin-2-one ($4A_1$-$4A_5$): To a solution of urea (2 mol) and chalcone (1 mol) in ethanol, conc. HCl (5 mL) was added and refluxed for 6 h. The completion of the reaction was monitored on a TLC plate. After completion, the reaction mixture was cooled to room temperature and neutralized with dil. NH_3 solution (10%) and refrigerated for 2 h (**Scheme-I**). The obtained solid product was filtered and washed thoroughly with water and recrystallized in an equimolar proportion of water and ethanol solvent [19].

4-Phenyl-6-[(1*E*)-2-phenylethenyl]-1,2,3,4-tetrahydropyrimidin-2-one ($4A_1$): Yield: 70%, m.p.: 302-304 ºC, *m.f.*: $C_{18}H_{16}N_2O$; *m.w.*: 276, R_f: 0.7. IR (ν_{max}, cm^{-1}): 3423 (N-H *str.*), 3055 (Ar C-H *str.*), 1627 (N-H *str.*), 1576 (C=O *str.*), 1497 (C=CH *str.*); ^{1}H NMR ($CDCl_3$, 800 MHz) δ ppm: 6.9-7.4 (m, 10H, arom. C-H), 6.9 (d, 1H, Hα), 8.2 (d, 1H, Hβ), 3.9 (dd, 1H, Ha), 6.95 (d, 1H, Hb), 6.04 (s, 1H, H-N1), 6.01 (s, 1H, H-N2); MS *m/z*: 277.13 $[M+H]^+$.

4-(4-Methoxyphenyl)-6-[(1*E*)-2-(4-methoxyphenyl)-ethenyl]-1,2,3,4-tetrahydropyrimidin-2-one ($4A_2$): Yield: 65%, m.p.: 348-350 ºC, *m.f.*: $C_{20}H_{20}N_2O_3$; *m.w.*: 336; R_f = 0.74. IR (ν_{max}, cm^{-1}): 3391 (N-H *str.*), 2998 (Ar C-H *str.*), 2924 (C=CH alkene *str.*), 1640 (N-H bend)1596 (C=O *str.*); ^{1}H NMR ($CDCl_3$, 800 MHz) δ ppm: 6.8-7.21 (m, 8H, Ar C-H), 6.7 (d, 1H, Hα), 8.3 (d, 1H, Hβ), 3.9 (dd, 1H, Ha), 7.2 (dd, 1H, Ha), 5.99 (s, 1H, H-N1), 6 (s, 1H, H-N2), 2.5 (s, 6H, OCH_3); MS *m/z*: 337.11 $[M+H]^+$.

4-(4-Fluorophenyl)-6-[(1*E*)-2-(4-fluorophenyl)ethenyl]-1,2,3,4-tetrahydropyrimidin-2-one ($4A_3$): Yield: 65%, m.p.: 394-396 ºC, *m.f.*: $C_{18}H_{14}N_2OF_2$; *m.w.*: 312; R_f = 0.5. 65; IR (ν_{max}, cm^{-1}): 3391 (N-H *str.*), 2998 (Ar C-H *str.*), 2924 (C=CH alkene *str.*), 1640 (N-H bend), 1596 (C=O *str.*), 1386.82 (C-F *str.*); ^{1}H NMR ($CDCl_3$, 800 MHz) δ ppm: 6.9-7.4 (m, 8H, Ar C-H), 6.8 (d, 1H, Hα), 8.5 (d, 1H, Hβ), 3.82 (dd, 1H, Ha), 6.6 (dd, 1H, Hb), 6.18 (s, 1H, H-N1), 6.19 (s, 1H, H-N2); MS *m/z*: 313.15 $[M+H]^+$.

4-(2-Chloro-6-fluorophenyl)-6-[(1*E*)-2-(2-chloro-6-fluorophenyl)ethenyl]-1,2,3,4-tetrahydropyrimidin-2-one ($4A_4$): Yield: 65%, m.p.: 327-329 ºC, *m.f.*: $C_{18}H_{12}N_2OF_2Cl_2$; *m.w.*: 380; R_f = 0.6. IR (ν_{max}, cm^{-1}): 3391 (N-H *str.*), 2998 (Ar C-H *str.*), 2924 (C=CH alkene *str.*), 1640 (N-H bend), 1596 (C=O *str.*), 1220.96 (C-F *str.*), 815.16 (C-Cl *str.*); ^{1}H NMR ($CDCl_3$, 800 MHz) δ ppm: 6.7-7.4 (m, 6H, Ar C-H), 6.6 (d, 1H, Hα), 8.5 (d, 1H, Hβ), 3.9 (dd, 1H, Ha), 6.25 (dd, 1H, Hb), 6.18 (s, 1H, H-N1), 6.16 (s, 1H, H-N2); MS *m/z*: 381.11 $[M+H]^+$.

4-(Thiophen-2-yl)-6-[(1*E*)-2-(thiophen-2-yl)ethenyl]-1,2,3,4-tetrahydropyrimidin-2-one ($4A_5$): m.f.: $C_{14}H_{12}N_2OS_2$; m.w.: 288; R_f = 0.4; m.p. (°C): 365-367; Yield (%): 65; IR (ν, cm^{-1}): 3391 (N-H *str.*), 2998 (Ar C-H *str.*), 2924 (C=CH alkene *str.*), 1640 (N-H bend), 1596 (C=O *str.*); ^{1}H NMR ($CDCl_3$, 800 MHz) (δ ppm): 6.4-7.4 (m, 14H, Ar C-H), 6.6 (d, 1H, Hα), 8.6 (d, 1H, Hβ), 4.21 (dd, 1H, Ha), 6.3 (dd, 1H, Hb), 6 (s, 1H, H-N1), 5.98 (s, 1H, H-N2); MS *m/z*: 289.41 $[M+H]^+$.

Prediction of physico-chemical, pharmacokinetic and ADMET studies: Using the SwissADME web platform, computational investigations of the synthesized compounds $4A_1$-$4A_5$ were carried out to forecast molecular characteristics. The synthesized compound's molecular weight, molecular volume, the logarithm of the partition coefficient, number of hydrogen-bond donors, number of hydrogen-bond acceptors, topological polar surface area, number of rotatable bonds and Lipinski's rule of five were all calculated.

Molecular docking studies: To evaluate the efficacy of the AutoDock 4.2.6 docking program, the crystal structures of human Eg5 motor domain bound to Mg-ADP and monastrol were employed in the current work. The Protein Data Bank was used to obtain the crystal structure of the human Eg5 motor domain in complex with its inhibitor monastrol (PDB ID: 1X88). Eg5 comprises two identical subunits (A and B). The A subunit of the enzyme protein was the only part of the investigation. The B-chain and the monastrol group along with water molecules and heteroatoms were eliminated and saved as pdb file. With the help of the discovery studio application, ligand molecules were designed, optimized and saved as in pdb format for docking experiments with AutoDock 4.2.6. Using AutoDock Tools 1.5.6, all flexible torsions of the resulting ligand molecules were defined and saved in the pdbqt format. For a subsequent docking technique, the prepared ligands served as input files. Using a Lamarckian genetic method, docking simulations were carried out utilizing AutoDock 4.2.6. A rigid protein and

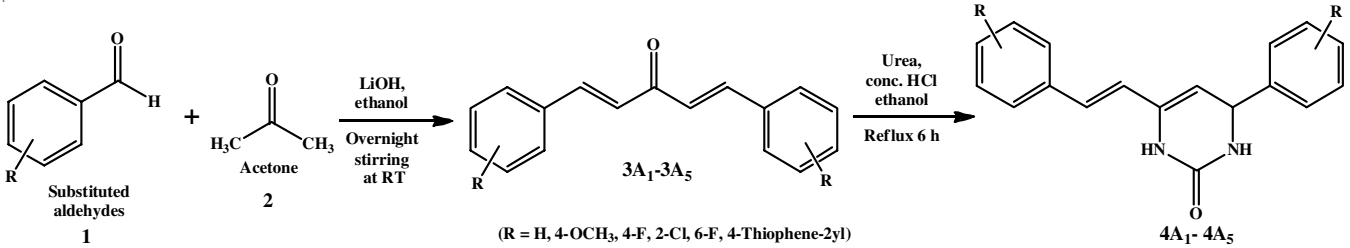

Scheme-I: Synthetic route of 4-phenyl-6-[(1*E*)-2-phenylethenyl]-1,2,3,4-tetrahydropyrimidin-2-one ($4A_1$-$4A_5$)

a flexible ligand with known torsion angles were docked using the standard approach (for 10 independent runs per ligand). According to the active pocket, a grid of 50, 50 and 50 points in x, y and z directions was modified. The energy map was calculated with a grid spacing of 0.375 Å. The Discovery studio visualization application was used to evaluate the resulting structural files.

Biological evaluation: The in *vitro* cytotoxicity studies on human breast cancer cell lines (MCF7 and MDA-MB-231) were used. The newly synthesized compounds (**$4A_1$** to **$4A_5$**) were screened for anticancer activity using the SRB assay method at Advanced Centre for Treatment, Research and Education in Cancer (ACTREC), Navi Mumbai (India). The synthesized compounds were evaluated by sulforhodamine B (SRB) assay. The experimental drugs were solubilized in appropriate solvents resulting in the final required drug concentrations of 10, 20, 40 and 80 µg/mL. The cell lines were grown in RPMI 1640 medium containing 10% fetal bovine serum and 2 mM L-glutamine. The cells were inoculated as per the assay conditions prior to the addition of experimental compounds. After the addition of experimental compounds, the plates were incubated under standard conditions. Sulforhodamine B (SRB) solution in acetic acid was added to each place and incubated for 20 min at room temperature. After staining, the unbound dye was recovered and residual dye was removed by washing with 1% acetic acid. The plates were air dried and the absorbance was read on a plate reader at a wavelength of 540 nm with a 690 nm reference wavelength. Percent growth was calculated on a plate-by-plate basis for test wells relative to control wells. Percent growth was expressed as (the ratio of average absorbance of the test well to the average absorbance of the control wells) × 100.

RESULTS AND DISCUSSION

A new series of dihydropyrimidinones was synthesized according to **Scheme-I**. Dibenzylideneacetone chalcones (**$3A_1$-$3A_5$**) were synthesized by Claisen-Schmidt condensation reaction between substituted aromatic aldehydes **1** and acetone **2** in presence of lithium hydroxide monohydrate ($LiOH·H_2O$) and ethanol as solvent. The synthesized chalcones were further reacted with urea in presence of conc. HCl and ethanol as solvent to yield desired dihydropyrimidinones (**$4A_1$-$4A_5$**). All the synthesized compounds were well characterized with FT-IR, ^{1}H NMR and mass spectroscopy.

The analytical data correlated with the proposed structure. The position of FT-IR bands provided the presence of the functional group. The structure of compound **$4A_1$** was confirmed by IR spectroscopy, the spectrum shows a strong absorption band due to the presence of the N-H stretch of dihydropyrimidinone ring in the region 3391 cm^{-1}. The aromatic C-H stretch was observed at 2998 cm^{-1} and aromatic C=CH stretch was observed at 2924 cm^{-1}. The amide (N-C=O) stretching vibration was observed at 1596 cm^{-1}. On the basis of their chemical shifts and multiplicities, the signals of the relevant protons of the synthesized derivatives were confirmed in the ^{1}H NMR spectra. The ^{1}H NMR spectra illustrated the sharp peaks in all compounds ranging from δ 7.9-7.0 ppm for aromatic protons. The H_a and H_b protons of the dihydropyrimidinone ring appeared as a doublet of the doublet. The doublet of H_a appeared at δ 6.9-6.6 ppm and doublets of H_b appeared at δ 7.6-7.2 ppm. The ^{1}H NMR spectra revealed a singlet at 8.6 and 4.9 ppm due to the two N-H protons. Mass spectroscopy was done for newly synthesized compounds. The M+1 peak was found for all compounds with respect to their molecular weight.

Physico-chemical, pharmacokinetic and ADMET properties: The ADME (absorption, distribution, metabolism and excretion) properties predict the therapeutic activity of small molecules based on their ability to reach the desired target at a sufficient concentration. The data predicted for the physicochemical characteristics, lipophilicity, solubility, pharmacokinetics and drug-likeness of synthesized compounds evaluated by the SwissADME online server are given in Table-1. The moieties **$4A_1$-$4A_5$** ranged in molecular weight from 276.3 to 414.1 g/mol and their clog P values fell within the permissible range of 2.00 to 5.00. The surface total of a molecule's polar atoms is known as the topological polar surface area (TPSA), all of the synthesized compounds had acceptable values between 20 and 130. It was predicted that all compounds would be mild to moderately soluble. For all compounds, the bioavailability score was 0.55 and anticipated to display desired drug-like qualities and be suitable for passive oral absorption based on Lipinski's rule of five, Muegge's filter, Veber's rule, Egan rule and Ghose filter except for compound **$4A_4$**.

A visual model called the Brain or Intestinal Estimated Permeation (BOILED-Egg) approach determines the polarity and lipophilicity of tiny compounds. The white region suggests a high probability of passive absorption by the gastrointestinal tract, whereas the yellow region suggests a strong likelihood of reaching the brain. Compounds **$4A_1$-$4A_4$**, with the exception of compound **$4A_5$**, were situated in the BBB region, exhibiting good BBB and gastrointestinal absorption, according to the BOILED-Egg diagram (Fig. 1). Compound **$4A_5$** solely demons-

TABLE-1
PHARMACOKINETICS AND DRUG-LIKENESS PREDICTIONS FOR THE SYNTHESIZED COMPOUNDS (**4A1- 4A5**) BY SwissADME

Code	MW[a]	HBA[b]	HBD[c]	TPSA[d]	Log P[e]	ESOL[f] class	GIA[g]	Lipinski #violations	Bioavailability score	P-gp[h] substrate	BBB[i] permeability
$4A_1$	276.33	1	2	41.13	2.75	Soluble	High	0	0.55	No	Yes
$4A_2$	336.38	3	2	59.59	3.36	Moderately soluble	High	0	0.55	No	Yes
$4A_3$	312.31	3	2	41.13	2.92	Moderately soluble	High	0	0.55	No	Yes
$4A_4$	381.2	3	2	41.13	3.19	Moderately soluble	High	1	0.55	No	Yes
$4A_5$	288.39	1	2	97.61	2.73	Soluble	High	0	0.55	No	No

[a]Molecular weight; [b]Hydrogen bond acceptors; [c]Hydrogen bond donors; [d]Topological surface area; [e]Octanol-water partition coefficient; [f]Solubility class; [g]Gastro-intestinal absorption; [h]P-glycoprotein; [i]Blood-Brain Barrier.

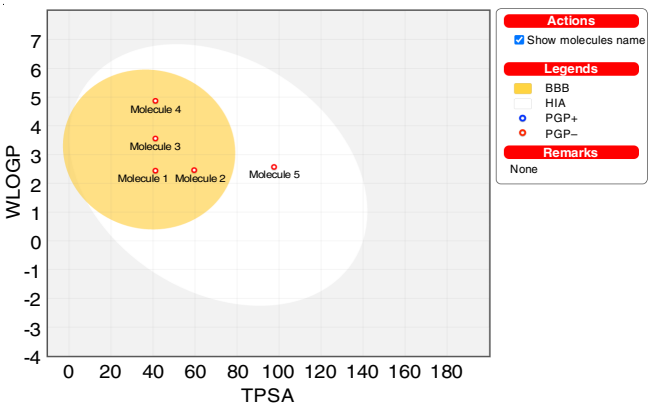

Fig. 1. BOILED-Egg graphical representation of the synthesized compounds and enzyme inhibition predictions

trated a good gastrointestinal absorption, whereas all compounds were estimated to be non-substrates for P-gp. The bioavailability (BA) radar plot provides a plausible profile of the oral bioavailability of compound, where the pink-coloured area of the radar plot is the supreme zone.

Molecular docking studies: According to the docking technique, molecules **$4A_1$-$4A_5$** were successfully docked in the active site of Eg5. The docking experiment's computed free energy of binding and inhibition constants are displayed in Table-2. The active site of the Eg5 enzyme was docked with ethyl 4-(3-hydroxyphenyl)-6-methyl-2-thioxo-1,2,3,4-tetrahydropyrimidine-5-carboxylate. A thorough examination of the binding pocket revealed that ethyl 4-(3-hydroxyphenyl)-6-methyl-2-thioxo-1,2,3,4-tetrahydropyrimidine-5-carboxylate (NAT) adopted a position with hydrophobic bonding surrounded by ALA133, PRO137 and hydrogen bonding by GLU116, GLY117, GLU118, ARG119 and TYR211 (Fig. 2).

The free binding energies of the proposed compounds range from -6.86 to -8.57 kcal/mol, while the free binding energy of the co-crystallized ligand (NAT) is -7.52 kcal/mol. Compared to the co-crystallized ligand's free binding energy, the free binding energies of compounds **$4A_1$** and **$4A_4$** were -8.30 and -8.57 kcal/mol, respectively. These compounds interact with amino acids by forming hydrogen bonds with GLU116, GLY117, GLU118, ARG119, TRP127 and TYR211 and by interacting hydrophobically with ALA133, PRO137, ARG221 and LEU214. The co-crystallized ligand (NAT) shows various interactions with amino acids *i.e.*, GLU116, GLY117, GLU118, ARG119, TR127, ALA133, PRO137, TYR211, LEU 214, ALA218 and ARG221 [18]. Similar interactions exist between the different amino acids and the co-crystallized ligand in the designed molecules. When compared to the co-crystallized ligand, the proposed compounds exhibit similar conformational and binding interactions. It implies that the synthesized compounds may have effective anti-proliferative activities.

TABLE-2
AUTODOCK ESTIMATED FREE ENERGIES OF BINDING, THE CALCULATED INHIBITION CONSTANTS (Ki) AND THE INTERACTIONS OF THE DESIGNED MOLECULES AND CO-CRYSTALLIZED LIGAND (TEMPERATURE = 298.15 K)

Compound code	Estimated free energy of binding	Estimated inhibition constant (Ki)	Interactions	
			H-Bonding	Hydrophobic bonding
$4A_1$	-8.30	819.36 nM	GLU116, GLY117	ARG221, ALA128, ARG119, PRO137, ALA133
$4A_2$	-6.86	9.32 µM	ARG119, ARG221, GLU116	ALA133, PRO137, ILE136, LEU160, ARG119, ARG221
$4A_3$	-7.63	2.54 µM	GLU116, GLY117, GLU118, TRP127	ARG221, PRO137, LEU214, ALA218, ARG221
$4A_4$	-8.57	526.87 nM	GLU118	GLU116, ARG221, LEU214, PRO137, ALA133, ARG119
$4A_5$	-7.54	2.97 µM	GLU116, GLY117, TRP127	-
Co-crystallized ligand (NAT)	-7.52	3.07 µM	GLU116, GLY117, GLU118, ARG119, TRP127, TYR211	ALA133, PRO137, LEU214, ALA218, ARG221

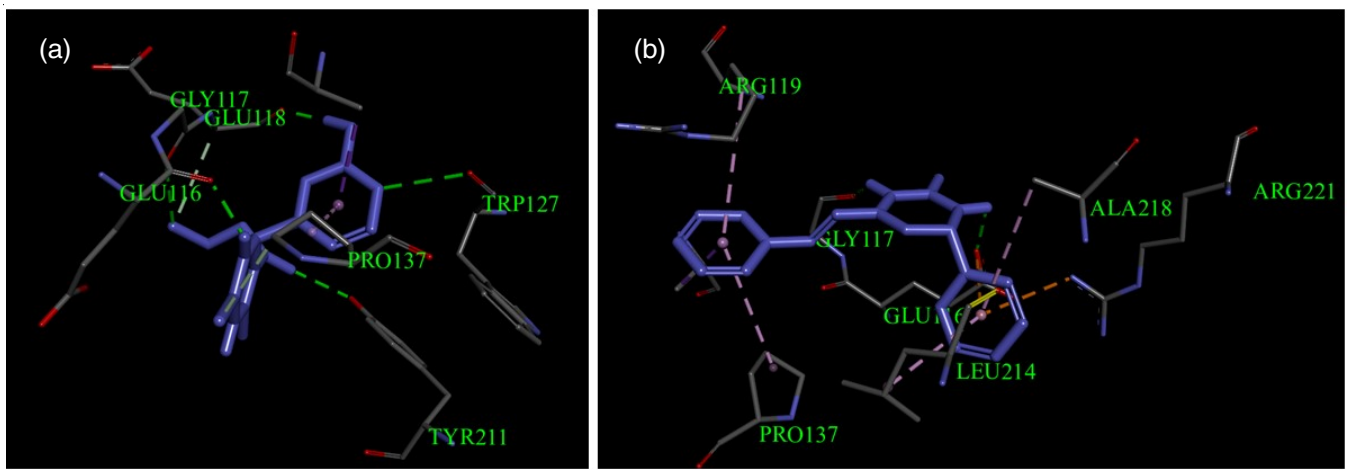

Fig. 2. (a) View of the Eg5 binding site surface from the PDB 1X88 structure showing the co-crystallized monastrol; (b) Docked view of compound **$4A_1$** on the active site of the Eg5 target

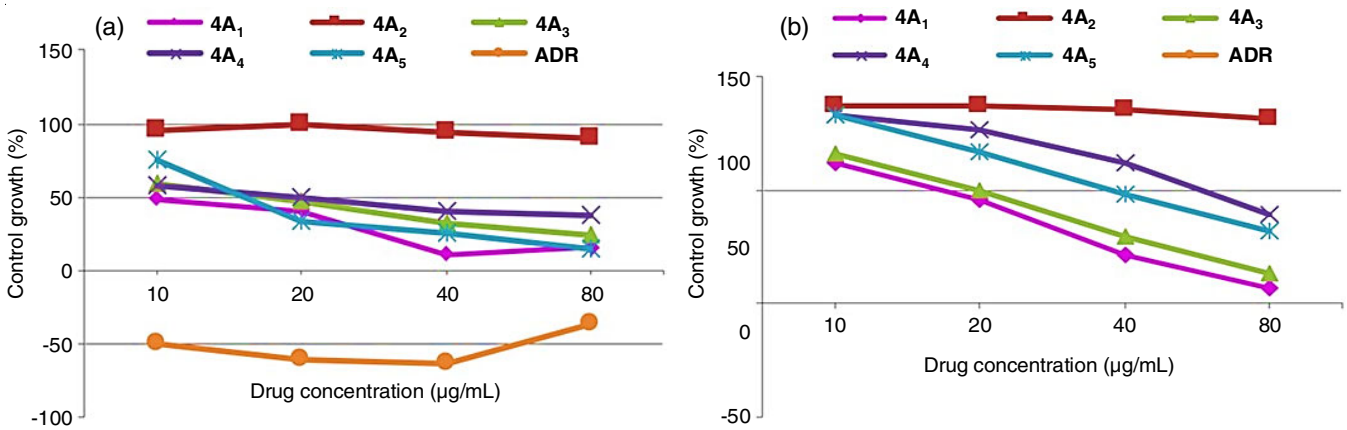

Fig. 3. Results obtained for the *in vitro* cytotoxicity activity of compounds on human breast cancer cell line (a) MCF7 and (b) MDB-MB-231

Biological Evaluation: After the successful synthesis of novel dihydropyrimidinone derivatives, they were evaluated for their biological activity against human breast cancer cell lines MCF7 and MDA-MB-231. The MCF7 cell line has a functional estrogen and EGF receptor and is dependent on estrogen and EGF for growth, it is uninvasive. On the other hand, MDA-MB-231 lacks ER and is unresponsive to estrogen. It provides a more aggressive and hormone-independent breast cancer cell line. All the synthesized compounds were tested for *in vitro* anticancer activity against human breast cancer cell line MCF7 and MDA-MB-231 using the SRB assay method. The results were obtained with respect to GI_{50} and defined as the concentration of drug causing 50% inhibition of cell growth.

As per NCI guidelines, a GI_{50} value of ≤ 10 µg/mL was considered to demonstrate highly significant inhibitory activity. Table-3 shows that the compounds produced exhibited adequate activity at lower doses. For the human breast cancer cell line MCF7, the growth curve graph and % control growth values displayed that compound **4A$_1$** was determined to be potent and active because it suppresses the growth of cells below 10 µg/mL concentration in contrast to standard Adriamycin, which also inhibits the growth of cells below this concentration (Fig. 3a). Contrarily, compound **4A$_2$** was shown to be ineffective because it needs a higher concentration (over 80 µg/mL) to inhibit the cellular proliferation. Compounds **4A$_3$**, **4A$_4$** and **4A$_5$** may be moderately active as they inhibit 50% of cell growth at a concentration of 17.5, 24.8 and 18.6 µg/mL, respectively.

Since, compounds **4A$_1$** and **4A$_3$** suppress more than 50% cell growth at concentrations of 15.9 µg/mL and 22.7 µg/mL, respectively, in the Growth Curve graph and % Control Growth values for the human breast cancer cell line MDA-MB-231, they may be moderately active (Fig. 3b). Compounds **4A$_2$**, **4A$_4$** and **4A$_5$** were determined to be inactive because a higher concentration was required to suppress cell growth by 50%.

TABLE-3
In vitro CYTOTOXICITY STUDIES ON TWO HUMAN BREAST CANCER CELL LINES

Compound code	GI_{50} (µg/mL)	
	MCF7	MDA-MB-231
4A$_1$	< 10	15.9
4A$_2$	> 80	> 80
4A$_3$	17.5	22.7
4A$_4$	24.8	62.0
4A$_5$	18.6	48.6
Adriamycin	< 10	< 10

Conclusion

In conclusion, dihydropyrimidinone derivatives (**4A$_1$-4A$_5$**) were successfully synthesized using partly green and conventional methods with better yields. The identification of compounds was established by single spot TLC, melting point and spectroscopic techniques involving FTIR, ^{1}H NMR and mass spectrometry. The newly synthesized compounds had drug-likeliness and demonstrated good BBB permeability and GI absorption. The synthesized molecules were successfully docked on the active site of Eg5 protein and showed similar interactions compared to the co-crystallized ligand (monastrol). It was observed that compound **4A$_1$** was found to have promising anticancer activity against human breast cell line MCF7 and MDA-MB-231. Additionally, it was also found that the newly synthesized compounds inhibited cell development whereas the standard (Adriamycin) killed the cells. While the compounds with the replacement of an electron-withdrawing group decreased activity, the molecule without any modification demonstrated good antiproliferative activity.

ACKNOWLEDGEMENTS

The authors are thankful to Dr. V.J. Kadam, Principal, Bharati Vidyapeeth's College of Pharmacy, Navi Mumbai, India for providing the research facilities during the course of the project.

CONFLICT OF INTEREST

The authors declare that there is no conflict of interests regarding the publication of this article.

REFERENCES

1. R. Kaur, S. Chaudhary, K. Kumar, M.K. Gupta and R.K. Rawal, *Eur. J. Med. Chem.*, **132**, 108 (2017); https://doi.org/10.1016/j.ejmech.2017.03.025

2. M.L.H. Santana, F.T. Masson, L.A. Simeoni and M. Homem-de-Mello, *Eur. J. Med. Chem.*, **143**, 1779 (2018); https://doi.org/10.1016/j.ejmech.2017.10.073
3. C.O. Kappe, *Acc. Chem. Res.*, **33**, 879 (2000); https://doi.org/10.1021/ar000048h
4. R. Soni, G. Singh, R. Kaur, G. Kaur, R.K. Gill and J. Bariwal, *Chem. Biol.*, **4**, 163 (2014).
5. M.M. Karelson, A.R. Katritzky, M. Szafran and M.C. Zerner, *J. Org. Chem.*, **54**, 6030 (1989); https://doi.org/10.1021/jo00287a012
6. V. Sarli and A. Giannis, *Clin. Cancer Res.*, **14**, 7583 (2008); https://doi.org/10.1158/1078-0432.CCR-08-0120
7. A. Blangy, H.A. Lane, P. d'Hérin, M. Harper, M. Kress and E.A. Niggt, *Cell*, **83**, 1159 (1995); https://doi.org/10.1016/0092-8674(95)90142-6
8. H.V. Goodson, S.J. Kang and S.A. Endow, *J. Cell Sci.*, **107**, 1875 (1994); https://doi.org/10.1242/jcs.107.7.1875
9. C.E. Walczak and T.J. Mitchison, *Cell*, **85**, 943 (1996); https://doi.org/10.1016/S0092-8674(00)81295-7
10. H. Wakui, N. Yamamoto, S. Kitazono, H. Mizugaki, S. Nakamichi, Y. Fujiwara, H. Nokihara, Y. Yamada, K. Suzuki, H. Kanda, S. Akinaga and T. Tamura, *Cancer Chemother. Pharmacol.*, **74**, 15 (2014); https://doi.org/10.1007/s00280-014-2467-z
11. S. Ding, N. Xing, J. Lu, H. Zhang, K. Nishizawa, S. Liu, X. Yuan, Y. Qin, Y. Liu, O. Ogawa and H. Nishiyama, *Int. J. Urol.*, **18**, 432 (2011); https://doi.org/10.1111/j.1442-2042.2011.02751.x
12. A. Masuda, K. Maeno, T. Nakagawa, H. Saito and T. Takahashi, *Am. J. Pathol.*, **163**, 1109 (2003); https://doi.org/10.1016/S0002-9440(10)63470-0
13. U. Soumyanarayanan, V.G. Bhat, S.S. Kar and J.A. Mathew, *Org. Med. Chem. Lett.*, **1**, 1 (2012).
14. U.T. Mayer, T.M. Kapoor, S.J. Haggarty, R.W. King, S.L. Schreiber and T.J. Mitchison, *Science*, **286**, 971 (1999); https://doi.org/10.1126/science.286.5441.971
15. M. Gartner, N. SunderPlassmann, J. Seiler, M. Utz, I. Vernos, T. Surrey and A. Giannis, *ChemBioChem*, **6**, 1173 (2005); https://doi.org/10.1002/cbic.200500005
16. R.R. Shinde and M. Farooqui, *Polycycl. Aromat. Compd.*, **42**, 6475 (2022); https://doi.org/10.1080/10406638.2021.1984262
17. C. Zhuang, W. Zhang, C. Sheng, W. Zhang, C. Xing and Z. Miao, *Chem. Rev.*, **117**, 7762 (2017); https://doi.org/10.1021/acs.chemrev.7b00020
18. S.D. Bajaj, O.A. Mahodaya and P.V. Tekade, *Int. J. Res. Biosci. Agric. Technol.*, **2**, 24 (2014).
19. A. Desai, K.B. Vyas, R.N. Patel and K.S. Nimavat, *Int. J. Pharm. Res. Scholars*, **2**, 1 (2016).